Published in final edited form as:
Biomacromolecules. 2012 October 8; 13(10): 3334–3342. doi:10.1021/bm301108x.

Dual Action Antimicrobials: Nitric Oxide Release from Quaternary Ammonium-Functionalized Silica Nanoparticles

Alexis W. Carpenter, **Brittany V. Worley**, **Danielle L. Slomberg**, and **Mark H. Schoenfisch***
Department of Chemistry, University of North Carolina at Chapel Hill, Chapel Hill, North Carolina 27599

Abstract

The synthesis of quaternary ammonium (QA)-functionalized silica nanoparticles with and without nitric oxide (NO) release capabilities is described. Glycidyltrialkylammonium chlorides of varied alkyl chain lengths (i.e., methyl, butyl, octyl, and dodecyl) were tethered to the surface of amine-containing silica nanoparticles via a ring-opening reaction. Secondary amines throughout the particle were then functionalized with *N*-diazeniumdiolates NO donors to yield dual functional nanomaterials with surface QAs and total NO payloads of ca. 0.3 μmol/mg. The bactericidal activities of singly (i.e., only NO-releasing or only QA-functionalized) and dual (i.e., NO-releasing and QA-functionalized) functional nanoparticles were tested against Grampositive *Staphylococcus aureus* and Gram-negative *Pseudomonas aeruginosa*. Particles with only NO release capabilities alone were found to be more effective against *P. aeruginosa*, while particles with only QA-functionalities exhibited greater toxicity toward *S. aureus*. The minimum bactericidal concentrations (MBC) of QA-functionalized particles decreased with increasing alkyl chain length against both microbes tested. Combining NO release and QA-functionalities on the same particle resulted in an increase in bactericidal efficacy against *S. aureus*; however, no change in activity against *P. aeruginosa* was observed compared to NO-releasing particles alone.

Keywords

nitric oxide release; diazeniumdiolate; quaternary ammonium; silica nanoparticle; antimicrobial; combination therapy

INTRODUCTION

With increasing occurrences of microbial antibiotic resistance,[1] alternative approaches for fighting infections have become necessary. Co-administering two antimicrobials that act via different mechanisms has been shown to significantly reduce microbial resistance and often results in synergy where the two agents are more effective in combination than when administered alone.[2, 3] As such, researchers are developing strategies to modify macromolecules (e.g., dendrimers, particles, polymers) with multiple antimicrobial agents.[4-6] For example, macromolecular vehicles have been designed to consist of a

*Corresponding Author schoenfisch@unc.edu.

Author Contributions The manuscript was written through contributions of all authors. All authors have given approval to the final version of the manuscript.

Supporting Information. XPS Spectra (Cl 2p), DLS size distribution and correlation data, DLV zeta potential distribution and phase plots, Zeta potential in protein-rich media, FT-IR spectra, and ^{1}H NMR spectra. This material is available free of charge via the Internet at http://pubs.acs.org

permanent antimicrobial characteristic that remains after the depletion of the releasable agent.[7]

Long chain quaternary ammoniums (QA) are a popular non-depleting antimicrobial component due to their broad-spectrum efficacy, simple structure, and ability to kill bacteria with no affect on the QA structure.[8] The positively charged ammonium group promotes direct interaction with the negatively charged bacterial membrane, causing chemical imbalances by replacing essential metal cations. Simultaneously, the long alkyl chain of QAs inserts into the membrane and cause physical damage. The simple structure of the QA functionalities allows for straight forward integration into polymers,[9, 10] films,[11-13] dendrimers,[14] and particles,[8, 15, 16] while still retaining their antimicrobial properties. Unfortunately, tethering QAs to polymers or particles limits their action to only those bacteria that come in direct contact with the macromolecule. Thus, coupling QA functionalities with a second releasable agent may increase the materials' sphere of influence and benefits from the advantages of the combination therapies discussed above. Indeed, QA-functionalized polymers impregnated with releasable silver ions (Ag^+) exhibited a wider zone of inhibition than QA polymers alone.[7, 17] Similarly, Wong et al. reported improved efficacy of QA-functionalized layer-by-layer coatings that leached gentamicin against biofilm formation.[18]

To date, most combination strategies have only been applied to polymeric coatings or films. Silica nanoparticles are well-poised for combination therapies due to their high surface area to volume ratio, chemical flexibility, and limited toxicity to mammalian cells.[19] Our laboratory has demonstrated the broad-spectrum bactericidal efficacy of silica nanoparticles that actively release nitric oxide (NO),[20-22] a gaseous molecule produced endogenously as part of the innate immune response.[23] Nitric oxide and its reactive byproducts decrease bacterial viability via both lipid peroxidation and reaction with membrane proteins, DNA, and metabolic enzymes.[23] The key advantage of employing NO over other releasable agents (e.g., silver and antibiotics) involves NO's multimodal antimicrobial activity and low toxicity to mammalian cells at concentrations necessary for antimicrobial action.[24] Furthermore, initial studies suggest the inability of bacteria to develop resistance to nanoparticle derived NO.[25] The potential of NO-based therapeutics is evident in the immense research efforts focused on designing NO-releasing macromolecular vehicles for biomedical applications. [26,27]

The storage of exogenous NO within silica nanoparticles is achieved by forming *N*-diazeniumdiolate NO donors on secondary amine sites incorporated within the silica network (Scheme 1).[22], 28 Upon exposure to physiological solution (pH 7.4, 37 °C), the *N*-diazeniumdiolates undergo proton-initiated decomposition to release two molecules of NO per secondary amine site. Moreover, the rate of NO release is dependent on the NO donor structure and chemical environment. We hypothesize that the incorporation of long chain quaternary ammoniums onto the surface of NO-releasing silica nanoparticles may result in increased efficacy compared to singly functionalized particles (i.e., QA or NO release alone). Herein, we investigated the role of QA alkyl chain length and NO release capability on the bactericidal efficacy against Gram-positive *Staphylococcus aureus* and Gram-negative *Pseudomonas aeruginosa.*

MATERIALS AND METHODS

Tetramethoxysilane and *N*-(6-aminohexyl)aminopropyltrimethoxysilane were purchased from Gelest (Morrisville, PA). Glycidyltrimethylammonium chloride, epichlorohydrin, dimethylbutylamine, dimethyloctylamine, dimethyldodecylamine, trimethylsilanolate, propidium iodide (PI), and benzalkonium chloride (BAC) were purchased from Sigma

Aldrich (St. Louis, MO). *N,N*-dimethylacetamide, methanol (anhydrous), ethanol, ammonia solution (30%) and tetrahydrofuran (anhydrous) were purchased from Fisher Scientific (Fair Lawn, NJ). Media and reagents for bacteria and mammalian cell assays were purchased from Becton, Dickinson and Company (Sparks, MD). *Pseudomonas aeruginosa* (P. aeruginosa) (ATCC #19143) and Staphylococcus aureus (S. aureus) (ATCC #29213) were obtained from American Type Tissue Culture Collection (Manassas, VA), and L929 mouse fibroblasts were obtained from the UNC Tissue Culture Facility (Chapel Hill, NC). 4,5-Diaminofluorescein diacetate (DAF-2 DA) was purchased from Calbiochem (San Diego, CA). Nitrogen (N2), argon (Ar), and nitric oxide calibration (26.81 PPM, balance N_2) gases were purchased from National Welders (Raleigh, NC). Pure nitric oxide gas (99.5%) used for N-diazeniumdiolate formation was purchased from Praxair (Sanford, NC). Distilled water was purified using a Millipore Milli-Q UV Gradient A-10 system (Bedford, MA), resulting in a total organic content of ≤6 ppb and a final resistivity of 18.2 mΩ·cm.

Synthesis of Amine-functionalized Silica Nanoparticles

The Stöber method was used to form monodisperse, spherical silica nanoparticles with amine functionalities throughout the particle as previously described.[29] Briefly, a premixed solution of *N*-(6-aminohexyl)aminopropyltrimethoxysilane (AHAP) (1.173 mL) and tetramethoxysilane (TMOS) (0.708 mL) was added to a solution of ethanol (59.16 mL), water (27.84 mL), and ammonium hydroxide (9.8 mL). The reaction was stirred at room temperature for 2 h. The resulting white particle precipitates were collected by centrifugation (3645*g*, 10 min, 4 °C) and washed thrice with ethanol to remove unreacted reagents. The particles were then dried in vacuo and stored in a sealed container at room temperature until further use.

Synthesis of Quaternary Ammonium-functionalized Silica Nanoparticles

The addition of QA functionalities to the particle surface involved the synthesis of quaternary ammonium epoxides (QA-epoxides) that were then subsequently reacted with primary amines on the particle via a ring-opening reaction (Scheme 1). To form the QA-epoxides, 0.04 mmol epichlorohydrin was reacted with 0.01 mmol *N,N*-dimethylbutylamine, *N,N*-dimethyloctylamine, or *N,N*-dimethyldodecylamine at room temperature overnight. The mixture was added dropwise to cold ether while sonicating, and the solid/viscous liquid QA-epoxides were collected via centrifugation (810*g*, 5 min). The supernatant containing excess epichlorohydrin and unreacted trialkylamines was decanted, 50 mL fresh cold ether was added, and the QA-epoxides were sonicated extensively. This washing procedure was repeated three times, followed by drying of the QA-epoxides in vacuo. The removal of unreacted epichlorohydrin and trialkylamines was confirmed with ^{1}H NMR. Glycidyldimethylbutylammonium chloride (butylQA) was a viscous liquid: ^{1}H NMR δ 0.98 (t, 3 H), 1.41 (m, 2H), 1.70 (m, 2H), 2.79 (dd, 1H), 2.98 (t, 1H), 3.24 (dd, 1H), 3.44 (s, 6H), 3.52 ppm (m, 1H), 3.63 ppm (dt, 2H), and 4.62 ppm (dd, 1H); ^{13}C NMR δ 13.8, 19.9, 25.5, 45.5, 45.3, 53.1, 65.4, and 66.9 ppm; ESI/MS m/z 158.09. Glycidyldimethyloctylammonium chloride (octylQA) was a tacky solid; ^{1}H NMR δ 0.87 (t, 3 H), 1.29 (m, 10 H) 1.71 (m, 2H), 2.74 (dd, 1H), 2.98 (t, 1H), 3.10 (dd, 1H), 3.49 (s, 6H), 3.54 (m, 1H), 3.67 (dt, 2H), and 4.96 ppm (dd, 1H); ^{13}C NMR δ 14.2, 22.9, 23.71, 26.6, 29.4, 32.02, 45.3, 45.5, 53.1, 65.8 and 66.9 ppm; ESI/MS m/z 214.16. Glycidyldimethyldodecylammonium chloride (dodecylQA) was a waxy solid; ^{1}H NMR δ 0.87 (t, 3 H), 1.27 ppm (m, 18H), 1.70 ppm (m, 2H), 2.74 ppm (dd, 1H), 2.98 ppm (t, 1H), 3.08 ppm (dd, 1H), 3.54 ppm (s, 6H), 3.58 ppm (m, 1H), 3.65 (dt, 2H), and 4.97 ppm (dd, 1H); ^{13}C NMR δ 14.2, 23.1, 23.7, 26.5, 29.5, 29.7, 29.8, 29.9, 32.38, 45.3, 45.5, 53.1, 65.4, and 66.9 ppm; ESI/MS m/z 270.25. The IR spectra were similar for all QA-epoxides with the exception of the intensity of the saturated C-H absorbance at 2919 and 2850 cm^{-1}, which increased with increasing alkyl chain length. IR (neat): 3019 cm^{-1} (methyl C-H), 2920 cm^{-1} (saturated C-H), 2850 cm^{-1} (saturated C-H),

1468 cm^{-1} (methyl C-H), 1267 cm^{-1} (epoxy ring), 972 (quaternary ammonium), 909 cm^{-1} (epoxy ring).

A ring opening reaction was subsequently performed between the QA-epoxides and the primary amines on the surface of the particles (Scheme 1). The amine-containing silica particles (AHAP, 100 mg) were suspended in 2.5 mL *N,N*-dimethylacetamide via sonication, and 20 μL triethylamine was added. The QA-epoxides were dissolved in 5 mL *N,N*-dimethylacetamide and added in excess to the particle suspension. Dissolution of glycidyltrimethylammonium chloride required heating while all other QA-epoxides dissolved readily. The reaction was heated to 110 °C and allowed to proceed overnight. The resulting QA-modified particles were collected via centrifugation (3645*g*, 10 min, 4 °C), washed thrice with ethanol and dried in vacuo.

N-Diazeniumdiolation of Silica Nanoparticles

Silica particles were loaded with NO by forming *N*-diazeniumdiolate NO donors on secondary amine sites (Scheme 2). Briefly, 20 mg of AHAP/TMOS or QA-modified AHAP/TMOS particles were suspended by sonication in 4 mL of tetrahydrofuran, and trimethylsilanolate was added in a 3.5-fold excess relative to secondary amines, as determined with elemental analysis.[30, 31] The particle suspensions were then placed in a 160 mL Parr general purpose stainless steel pressure vessel with magnetic stirring and connected to an in-house NO reactor. The solutions were flushed 6 times with Ar to remove oxygen from the system, then pressurized to 10 bar with NO that had been scrubbed with KOH. The pressure was maintained at 10 bar for 3 d, after which it was released and the solutions were again purged with Ar to remove unreacted NO. The resulting *N*-diazeniumdiolate-modified silica nanoparticles were collected by centrifugation (3645*g*, 10 min, 4 °C), washed twice with a 50:50 (v/v) mixture of 5 mM NaOH and methanol to remove unreacted base and byproducts from the particle suspension. The NO-loaded particles were then washed twice with ethanol and dried in vacuo.

Nitric Oxide Release Measurements

Real-time NO release in deoxygenated PBS (pH 7.4) at 37 °C was monitored using Sievers NOA 280i chemiluminescence NO analyzer (NOA, Boulder, CO) connected to a customized reaction cell as described previously.[32] The absence of nitrite byproducts was confirmed by ensuring that total NO concentrations measured from both the Griess assay and the NOA were equal.[33] Prior to analysis, the NO analyzer was calibrated with air passed through a NO zero filter (0 ppm NO) and a 26.39 ppm NO standard gas (balance N_2).

Nanoparticle Characterization

The particles' zeta potentials (i.e., surface charge) were measured using a Malvern Zetasizer Nano-ZS equipped with a 10 mW HeNe laser (633 nm) and a NIBS® detector at an angle of 173°. All samples were prepared at 0.5 mg/mL concentrations in either 10 mM NaOH, 10 mM phosphate buffer or 1 vol% TSB in 10 mM phosphate buffer, sonicated briefly and analyzed at 37 °C. Phosphate buffer (non-saline, pH 7.4) was employed for zeta potential measurements to mimic the media used for bactericidal assays because the high ionic contents of phosphate buffered saline were found to corrode the folded capillary electrodes.[34] Particle size and morphology were characterized using a Hitachi S-4700 Scanning Electron Microscope (Pleasanton, CA). Carbon, hydrogen and nitrogen content were determined on a Perkin Elmer CHN/S elemental analyzer operating in CHN mode. X-ray photoelectron spectroscopy (XPS) analysis was performed on a Kratos Axis Ultra DLD X-ray Photoelectron Spectrometer with a monochromatic Al Kα X-ray source (150W). Electrons were collected at an angle of 90 degrees from the sample surface from a 300 × 700 μm area on the sample. The pass energy was set to 20 eV to allow for high resolution

spectra to be obtained. All spectra were obtained with a step size of 0.1 eV and calibrated to the C1s peak at 284.6 eV.

Bactericidal Assays

P. aeruginosa and *S. aureus* were cultured in tryptic soy broth to a concentration of 10^8 colony forming units per mL (CFU/mL), collected by centrifugation, and resuspended in PBS or 1% glucose, 0.5% TSB in PBS, respectively. Of note, *S. aureus* was not viable in PBS alone after 24 h. Each bacteria was diluted to 10^6 CFU/mL and treated with the appropriate concentration of QA-modified, NO-releasing, or NO-releasing QA-functionalized silica nanoparticles or BAC. Untreated controls (blanks) were included in each MBC experiment to ensure untreated bacteria remained viable (at 10^6 CFU/mL) over the 24 h incubation period. The samples were briefly sonicated and vortexed in order to suspend the particles. After 24 h of incubating at 37 °C, the particle-treated bacteria were spiral plated at 10- and 100-fold dilutions on tryptic soy agar plates. Bacterial viability was assessed by counting the number of colonies formed on the agar plate using a Flash & Go colony counter (IUL, Farmingdale, NY). Minimum bactericidal concentrations (MBC) were determined to be the minimum concentration of particles or BAC that reduced the bacteria colony counts from 10^6 to 10^3 CFU/mL (i.e., 3-log reduction). The plate counting method used herein has an inherent limit of detection of 2.5×10^3 CFU/mL.[35]

Confocal Microscopy for Detection of Intracellular NO and Cell Death

S. aureus was cultured in TSB to a concentration of 1×10^8 cfu/mL, collected via centrifugation (3645g, 10 min), resuspended in sterile PBS, and adjusted to 1×10^6 cfu/mL in PBS supplemented with 10 μM DAF-2 DA and 30 μM PI. Aliquots of the *S. aureus* solution were incubated in a glass bottom confocal dish for 45 min at 37 °C. A Zeiss 510 Meta inverted laser scanning confocal microscope with a 488 nm Ar excitation laser (2.0%) and a BP 505–530 nm filter was used to obtain DAF-2 (green) fluorescence images. A 543 nm HeNe excitation laser (25.3%) with a BP 560–615 nm filter was used to obtain PI (red) fluorescence images. The bright field and fluorescence images were collected using a N.A. 1.2 C-apochromat water immersion lens with a 40× objective. Suspensions (1.5 mL) of AHAP/NO (1 mg/mL) or dodecylQA-AHAP/NO (1 mg/mL) particles in PBS (supplemented with 10 μM DAF-2 DA, 30 μM PI) were sonicated and immediately added to the *S. aureus* solution (1.5 mL) in the glass confocal dish. Images were collected every 5 min to observe intracellular NO concentrations and bacteria cell death.

In Vitro Cytotoxicity

L929 mouse fibroblasts were grown in DMEM supplemented with 10% (v/v) fetal bovine serum (FBS) and 1 wt% penicillin/streptomycin, and incubated in 5% (v/v) CO_2 under humidified conditions at 37 °C. After reaching 80% confluency, the cells were trypsinized, seeded onto tissue culture treated polystyrene 96-well plates at a density of 3×10^4 cells/mL and incubated at 37 °C for 48 h. The supernatant was then aspirated and replaced with 200 μL fresh DMEM and 50 μL of either control (AHAP, methylQA, butylQA, octylQA, dodecylQA) or NO-releasing (AHAP/NO, methylQA/NO, butylQA/NO, octylQA /NO, dodecylQA/NO) nanoparticle suspensions in PBS at the determined MBCs against *P. aeruginosa* or *S. aureus*. After incubation at 37 °C for 24 h, the supernatant was aspirated and 120 μL mixture of DMEM/MTS/PMS (105/20/1, v/v/v) was added to each well. After 1.5 h incubation at 37 °C, the solution in each well was transferred to a microcentrifuge tube and centrifuged for 2 minutes to remove the silica particles. Ninety microliters (90 μL) of the supernatant was then added to a clean microtiter plate, and the absorbance of the colored solutions was quantified at 490 nm using a Thermoscientific Multiskan EX plate reader. The mixture of DMEM/MTS/PMS and untreated cells were used as blank and control, respectively. The cell viability was calculated by taking the ratio of the absorbance of treated

cells to the absorbance of untreated cells after subtracting the absorbance of the blank from both.

RESULTS AND DISCUSSION

Nanoparticle Synthesis and Characterization

We have previously reported the synthesis of amine-functionalized silica particles capable of variable NO storage and release characteristics.[22, 28, 36] For this study, particles were synthesized by hydrolyzing and co-condensing *N*-(6-aminohexyl)aminopropyltrimethoxysilane (AHAP) and tetramethoxysilane (TMOS) via a modified Stöber process. *N*-(6-aminohexyl)aminopropyltrimethoxysilane was selected as the NO-donor precursor due to its suitability for tethering QA-functionalities via primary amines. The AHAP particles employed in this study were characterized by a spherical morphology and diameters of 180±26 nm as determined by scanning electron microscopy (Figure 1A). Dynamic light scattering (DLS) analysis indicated that the particles were monodisperse with a polydispersity index (PDI) of 0.07±0.02 and a measured Z-average (190±7 nm), consistent with diameters observed with SEM. Employing a monodisperse particle system is important for studying antimicrobial efficacy as particle size has been shown to impact bactericidal activity.[22]

The AHAP silica particles were modified with QA functionalities via a ring-opening reaction between surface primary amines and QA-epoxides (Scheme 1). While glycidyltrimethylammonium chloride is commercially available, earlier work demonstrated optimal bactericidal efficacy with long chain QAs.[9, 37, 38] Quaternary ammonium-epoxides containing longer alkyl chains were thus synthesized by reacting epichlorohydrin with dimethylbutylamine, dimethyloctylamine, or dimethyldodecylamine (Scheme 1). The formation of the QA epoxides was confirmed with ^{1}H and ^{13}C NMR, IR spectroscopy, and ESI mass spectrometry (Supporting Information). A shift in the ^{1}H NMR resonances corresponding to the protons alpha to Cl/N and those of the nitrogen bound methyl groups confirmed the formation of the QA epoxide. Infrared absorbance bands indicating the QA-epoxide structure were also observed at 970 cm^{-1} (QA),[39] 1267 cm^{-1} (epoxide ring), and at 2920 and 2850 cm^{-1} (saturated CH). The intensity of the saturated CH absorbance increased with the increase in the length of the alkyl chain.

The addition of QA groups to the particle surface was confirmed by monitoring changes in the nitrogen environments (N 1s) using X-ray photoelectron spectroscopy (XPS). As shown in Figure 2A, the N 1s peak for unmodified AHAP particles was fit with two component peaks at binding energies of 399 and 400 eV, corresponding to primary and secondary amines, respectively. The N 1s peak of QA-functionalized particles consisted of a third component at 402 eV, representing the quaternary ammonium (Figure 2B–E).[40] The R_4N^+ peak was most intense for the methylQA modified particles. The presence of a peak at 399 eV for all QA-functionalized particles indicates that not all primary amines at the particle surface were functionalized. Of note, a doublet at 198 eV was also observed for the QA-functionalized particles (Supporting Information), signifying the presence of the chloride counter ion. As expected, the synthetic strategy for QA surface modification did not influence particle size or morphology (Figure 1B–E).

Quaternary ammonium functionalization was also verified by observing changes in the zeta potentials between AHAP and QA-modified AHAP particles using laser doppler velocimetry (LDV). In 10 mM phosphate buffer PB, both unmodified AHAP and QA-modified particles exhibited a positive zeta potential due to the presence of protonated primary amines or positively charged QAs, respectively. In contrast, the zeta potential for the unmodified AHAP particles became negative in basic media (10 mM NaOH), whereas

the QA-functionalized particles remained positively charged (Table 1), indicating the presence of a permanent, pH independent positive charge. A slight decrease in the zeta potential for longer chained QA-modified particles was observed with increasing pH, which was also accompanied by a decrease in the derived count rates. Since all samples were prepared at the same concentration using similarly sized particles, the decrease in the derived count rate indicates sedimenting particles,[41] an expected phenomenon for more hydrophobic particles. Of note, the derived count rate and zeta potential of methylQA particles did not change regardless of pH. Overall, the larger count rates for the QA-modified particles in 10 mM NaOH suggest the positively charged particles are more stabilized in basic solution due to an abundance of negatively charged ions supporting the Stern layer.[41]

Nitric Oxide Release Analysis

The silica particles were exposed to high pressures of NO in the presence of a base to form *N*-diazeniumdiolates NO donors (i.e., NONOates) on the secondary amines. As shown in Figure 2, NONOate formation was confirmed by an absorbance maximum at 253 nm.[20] Figure 2 also depicts the absorbance from non-NO-releasing dodecyl-QA-modified AHAP, indicating the absence of the peak at 253 nm prior to exposure to NO. Of note, no absorbance maximum is present at 450 nm following exposure to NO, indicating the particles are free of cytotoxic nitrosamines.[42]

Nitric oxide storage and delivery was evaluated by monitoring NO production in real time via chemiluminescence. The addition of QA-functionalities did not influence the amine to NONOate conversion as each system released similar NO payloads of ca. 0.3 μmol/mg (Table 2). As such, the role of QA alkyl chain length on bactericidal efficacy could be elucidated since NO release remained constant. The Griess assay was used to confirm that no nitrite was formed during the NONOate reaction and NO liberation.[33] As is typical for NONOate-based silica particles,[28, 36] the real-time NO release profiles exhibited a maximum instantaneous NO concentration ($[NO]_{max}$) that was achieved shortly after the particles were introduced into the solution. The unmodified AHAP/NO and methylQA/NO were characterized as having similar $[NO]_{max}$ values (1388±161 and 1034±32 ppb/mg, respectively), whereas butylQA/NO, octylQA/NO, and dodecyl/NO had lower $[NO]_{max}$ (882±36, 791±52, 617±68 ppb/mg, respectively). The decrease in $[NO]_{max}$ with increasing alkyl chain may be attributed to the increased surface hydrophobicity that slows the rate of water diffusion into the particle. Such behavior was further demonstrated by an increase in the time to reach $[NO]_{max}$ (i.e., t_{max}) with increasing QA alkyl chain length. The NO payloads for each particle system were completely depleted by 24 h.

Bactericidal Efficacy

S. aureus and *P. aeruginosa* are two of the most commonly isolated species in chronic wounds and were therefore selected as the test microbes to evaluate the efficacy of the QA-functionalized nanoparticles presented herein.[43] We sought to test our nanoparticles against both Gram-positive (*S. aureus*) and Gram-negative (*P. aeruginosa*) bacteria strains as previous work has shown that the potency of both NO- and QA-based antimicrobials depend greatly on the bacterial membrane composition.[14, 44] Prior to evaluating the bactericidal activity of the dually functional nanoparticles, the efficacy of the monofunctional formulations alone (i.e., NO-releasig or QA-functionalized) were evaluated to fully understand the benefit of designing a combination approach.

The AHAP/NO particles proved to be significantly more effective against *P. aeruginosa* compared to *S. aureus* with MBC_{24h} of 1.5 and 3.5 mg/mL, respectively (Figure 4). These results are consistent with previously reported *N*-diazeniumdiolate based NO-releasing

nanoparticles.[21] Conversely, the antimicrobial activity of the QA-functionalized particles was greater against *S. aureus* than *P. aeruginosa* (Figure 4). Chen et al. also reported greater sensitivity of Gram-positive bacteria to QA-based antimicrobials compared to Gram-negative bacteria.[14] As shown in Figure 4, the methylQA particles did not present appreciable toxicity to either of the microbes tested. As expected, the bactericidal efficacy of QA-modified particles exhibited a strong dependence on alkyl chain length. Increasing the alkyl chain length from methyl to butyl, octyl and dodecyl resulted in a decrease in MBC_{24h} from 4.0, 3.0 and 1.5 mg/mL against *S. aureus*, respectively. OctylQA and dodecylQA particles were equally effective against *P. aeruginosa* and more effective than the butylQA particles. Antimicrobial activity of short chained QAs results from the positively charged ammonium group complexing with the negatively charged bacterial cell membrane to disrupt membrane functions, alter the balance of essential ions (i.e., K^+, Na^+, Ca^{2+}, and Mg^{2+}), interrupt protein activity, and damage bacterial DNA.[45] Long alkyl chain QAs can exert additional antimicrobial activity by inserting into the bacterial membrane, resulting in physical disruption.[45] Indeed, longer alkyl chains have been shown to be more effective due to deeper penetration into the membrane and concomitant disruption.[9, 37, 38] As a positive control, the bactericidal efficacy of benzalkonium chloride (BAC), a QA salt, was also determined under the assay conditions used herein. Benzalkonium chloride was chosen as a control as it is a long chained QA salt used as a commercial antiseptic. The MBC_{24h} doses of BAC against *S. aureus* and *P. aeruginosa* were 4 and 16 μg/mL, respectively. The lower doses of BAC required to induce a 3 log reduction compared to QA-modified particles are attributed to the macromolecular structure having an inherently larger mass due to the silica backbone. Moreover, the immobilization of the QAs onto the particle surface suggests their antimicrobial mechanisms differ from those of long chain QA salts that readily diffuse through cell membranes. The mechanism of action of QAs tethered to polymer surfaces has been proposed to depend strongly on the disruption of electrolyte equilibrium and less strongly on alkyl chain length.[11] However, the structure-dependent antimicrobial activity of the QA particles presented here suggests their antimicrobial mechanism may involve penetration into the cell membrane. OctylQA and dodecylQA particles were characterized by a negative zeta potential in 1 vol% TSB in PBS due to the likely adhesion of proteins to the particle surface (Supporting Information). These results indicate that the positive charge of the QA functionalities plays less of a role in their bactericidal activity.

The advantages of combining antimicrobial strategies on the same particle have previously been demonstrated with QA-functionalized surfaces that release an antimicrobial agent, such as silver ion[7, 17] or gentamicin.[18] Although these releasable therapies are potent antimicrobials, resistance concerns plaque their wide-spread use.[46, 47] The QA-functionalized particles described herein were designed to allow for the release of NO, a broad-spectrum antimicrobial with low risk of resistance.[25] As shown in Figure 4, NO-releasing long chain (i.e., octyl and dodecyl) QA-functionalized particles exhibited increased toxicity against *S. aureus* compared to particles functionalized with short chain (i.e., methyl or butyl) QAs or NO release alone. Nitric oxide-releasing AHAP/NO, methylQA/NO, and butylQA/NO were equally effective against *S. aureus* with an MBC_{24h} of 3.5 mg/mL. Increasing the alkyl chain length of NO-releasing QA particles to octyl and dodecyl improved the antimicrobial activity with a substantial decrease in MBC_{24h} to 1.5 and 1.0 mg/mL, respectively. Disruption of the bacterial membrane by the long chain QAs may allow for greater oxidative stress due to increased intracellular NO levels compared to treatment with AHAP/NO.[44] The combination of NO release and QA modification (i.e., NO-releasing QA-functionalized particles) did not alter the antimicrobial efficacy against *P. aeruginosa* compared to unfunctionalized NO-releasing particles (i.e., AHAP/NO). These results reflect those of the monofunctional particles, where the MBC_{24h} of dodecylQA was much greater than that of AHAP/NO against *P. aeruginosa*.

To prove the advantage of co treatment with QA-functionalized NO-releasing particles, we treated *S. aureus* and *P. aeruginosa* to 25% of the MBC_{24h} values of dodecylQA and AHAP/NO either simultaneous or at 30 min intervals. Sublethal doses were used to avoid complete killing and allow for viable enumeration, and short exposure intervals were used to inhibit the production of new or repaired cells.[44] As shown in Figure 5, the simultaneous addition of the two separate antimicrobial particles resulted in greater antimicrobial action against *S. aureus* than when the microbes were exposed to one agent (e.g., AHAP/NO or dodecylQA) followed by the second 30 min later. In comparison, the decrease in *P. aeruginosa* viability was the same for all combination treatments regardless of the addition order. These latter results were not surprising as the antimicrobial activity of NO-releasing dodecylQA was equal to that of NO-releasing AHAP/NO against *P. aeruginosa*.

Confocal microscopy was used to study the antimicrobial mechanisms of NO-releasing dodecylQA/NO particles against *S. aureus*. DAF-2, a green fluorescent marker for intracellular NO, and PI, a red fluorescent marker for a compromised membrane, were used to visualize the effects of the NO-release particles on the bacteria. As shown in Figure 7, treatment with dodecylQA/NO resulted in red fluorescence and weak green fluorescence after 60 min. Conversely, treatment with AHAP/NO for the same time period resulted in strong green fluorescence due to DAF without the presence of red fluorescence. Thus, the QA-functionalities were observed to cause membrane disruption, even before significant intracellular NO concentrations were achieved. As expected, the intensity of the green fluorescence increased with incubation time, indicating elevation of the intracellular NO concentrations. Moreover, the faster release kinetics of AHAP/NO compared to dodecylQA/NO resulted in greater intracellular NO concentrations at shorter exposure times.

Small differences in the physical and chemical properties of nanomaterials have been shown to greatly influence nanoparticle-cell interactions,[48] suggesting that the use of dual function nanoparticles may be more favorable than co-administering two different monofunctional nanoparticles. To investigate the validity of this hypothesis, the MBC_{24h} of a mixture of dodecylQA and AHAP/NO (50:50 w/w) particles was also determined. The MBC_{24h} of the dodecylQA+AHAP/NO particle mixture was 2.0 and 3.0 mg/mL against *S. aureus* and *P. aeruginosa*, respectively. The NO and QA concentrations of the 50:50 dodecylQA+AHAP/NO mixture correspond to the same NO and QA concentrations delivered from the MBC_{24h} doses of dodecylQA/NO (i.e., 1.0 and 1.5 mg/mL, respectively). Thus, combining NO release and QA-functionalities on the same particle proved advantageous as a lower total dose of particles was required to induce bactericidal efficacy compared to treatment with a mixture of two monofunctional particles.

In Vitro Cytotoxicity

The ultimate utility of next generation antimicrobials is often governed by their toxicity to mammalian cells, assuming adequate microbial killing. Although long chain quaternary ammonium salts have long been used clinically, they are mostly restricted to topical applications due to their toxicity against mammalian cells.[38, 49] However, tethering QAs to a macromolecules has been shown to decrease their toxicity toward eukaryotic cells.[49] We thus evaluated the toxicity of QA- and NO-releasing QA-functionalized particles against L929 fibroblasts cells (Figure 7). Fibroblast cells represent the standard for cytotoxicity screening of new antimicrobials due to their involvement in wound healing and the immune response.[50, 51] The viability of fibroblasts cells was monitored via the MTS assay following 24 h exposure to the MBC_{24h} against both *S. aureus* and *P. aeruginosa*. Control AHAP particles exhibited significant toxicity at the high particle dose of 6.0 mg/mL due to the presence of primary amines.[21, 52] Conversion of the primary amines to trimethylQA groups caused a significant decrease in the observed cytotoxicity, as 8 mg/mL of methylQA particles only decreased viability by 40%. The cytotoxicity of QA-functionalized particles

against fibroblasts at their MBC increased with increasing alkyl chain length. For example, 4.0 mg/mL butylQA, octylQA or dodecylQA-modified particles resulted in a 45, 60, and 94% decrease in viability, respectively. Fibroblast viability was decreased by 21 and 86% upon treatment with 4 and 16 μg/mL BAC. The cytotoxic effects observed even at significantly lower BAC concentrations indicate the advantage of particle bound QAs.

Due to the lower concentrations of particles required for microbial killing with NO-release, the cytotoxicity of NO-releasing QA-particles against fibroblast was notably less. For example, 4.0 mg/mL dodecylQA (MBC_{24h} against *P. aeruginosa*) resulted in a 94% decrease in fibroblast viability, while the MBC_{24h} dose of dodecylQA/NO (1.5 mg/mL) decreased fibroblast viability by only 69%. Moreover, the cytotoxicity of dodecylQA/NO was lower than that of BAC alone at the *P. aeruginosa* MBC. These results indicate that although no synergistic effects were observed for the dodecylQA/NO system, the coupling of QA-functionalities and NO release on the same particle may be advantageous as lower doses (particle concentrations) could be used to achieve bactericidal activity with less impact to mammalian cells.

CONCLUSIONS

Quaternary ammonium (QA)-functionalized particles exhibited antimicrobial action against both *S. aureus* and *P. aeruginosa*, with long alkyl-chain QAs (e.g., octyl and dodecyl) proving more potent than short alkyl-chain QAs (e.g., methyl and butyl). The functionalization of particles with both QA groups and NO donors resulted in particles with even more favorable antimicrobial activity against *S. aureus* compared to monofunctional QA-functionalized or NO-releasing particles alone. Conversely, the antimicrobial activity of the hybrid particles against *P. aeruginosa* was unchanged relative to the NO-releasing only particles. Overall, *S. aureus* was more sensitive to QA particle treatment, while the inverse was true for *P. aeruginosa* (greater sensitivity to NO). In addition, hybrid NO release/QA-functionalized particles proved to be more effective at microbial killing than mixtures of NO-releasing and QA-functionalized particles. The design of materials expressing multiple antimicrobial mechanisms of action may represent an important strategy for lowering the concentration of therapy required and reducing the risk of potential resistance.

Supplementary Material

Refer to Web version on PubMed Central for supplementary material.

Acknowledgments

This work was supported in part by the National Institutes of Health (NIH EB000708) and the National Science Foundation (DMR 1104892). A.W.C. gratefully acknowledges a graduate research fellowship from Eastman Chemical Company (Kingsport, TN). The authors thank Carrie Donley for assistance with XPS and Amar Kumbhar for assistance with SEM. We also acknowledge support for the purchase of instrumentation (FTIR) from UNC EFRC Center for Solar Fuels, an Energy Frontier Research Center funded by the U.S. Department of Energy, Office of Science, Office of Basic Energy Sciences under Award Number DE-SC0001011) and from UNC SERC ("Solar Energy Research Center Instrumentation Facility" funded by the US Department of Energy – Office of Energy Efficiency & Renewable Energy under Award Number DE EE0003188).

REFERENCES

(1). Coates A, Hu YM, Bax R, Page C. Nat. Rev. Drug Discov. 2002; 1:895–910. [PubMed: 12415249]

(2). Fischbach MA. Curr. Opin. Microbiol. 2011; 14:519–523. [PubMed: 21900036]

(3). Allahverdiyev AM, Kon KV, Abamor ES, Bagirova M, Rafailovich M. Exp. Rev. Anti. Infect. Ther. 2011; 9:1035–1052.

(4). Mintzer MA, Dane EL, O'Toole GA, Grinstaff MW. Mol. Pharmaceut. 2012; 9:342–354.
(5). Huh AJ, Kwon YJ. J. Control. Release. 2011; 156:128–145. [PubMed: 21763369]
(6). Tashiro T. Macromol. Mater. Eng. 2001; 286:63–87.
(7). Li Z, Lee D, Sheng X, Cohen RE, Rubner MF. Langmuir. 2006; 22:9820–9823. [PubMed: 17106967]
(8). Dong H, Huang J, Koepsel RR, Ye P, Russell AJ, Matyjaszewski K. Biomacromolecules. 2011; 12:1305–1311. [PubMed: 21384911]
(9). Jiang S, Wang L, Yu H, Chen Y. React. Funct. Polym. 2005; 62:209–213.
(10). Yao C, Li X, Neoh KG, Shi Z, Kang ET. J. Membr. Sci. 2008; 320:259–267.
(11). Huang J, Koepsel RR, Murata H, Wu W, Lee SB, Kowalewski T, Russell AJ, Matyjaszweski K. Langmuir. 2008; 24:6785–6795. [PubMed: 18517227]
(12). Oosterhof JJH, Buijssen KJDA, Busscher HJ, van der Laan BFAM, van der Mei JC. Appl. Environ. Microbiol. 2006; 72:3673–3677. [PubMed: 16672516]
(13). Majumdar P, Crowley E, Htet M, Stafslien SJ, Daniels J, VanderWal L, Chisholm BJ. ACS Comb. Sci. 2011; 13:298–309. [PubMed: 21480666]
(14). Chen CZ, Beck-Tan NC, Dhurjati P, van Dyk TK, LaRossa RA, Cooper SL. Biomacromolecules. 2000; 1:473–480. [PubMed: 11710139]
(15). Song J, Kong H, Jang J. Colloids Surf. B. 2011; 82:651–656.
(16). Beyth N, Yudovin-Farber I, Perez-Davidi M, Domb AJ, Weiss EI. Proc. Natl. Acad. Sci. U.S.A. 2010; 107:22038–22043. [PubMed: 21131569]
(17). Song J, Kang H, Lee C, Hwang SH, Jang J. ACS Appl. Mater. Interfaces. 2012; 4:460–465. [PubMed: 22181053]
(18). Wong SY, Moskowitz JS, Veselinovic J, Rosario RA, Timachova K, Blaisse MR, Fuller RC, Klibanov AM, Hammond PT. J. Am. Chem. Soc. 2010; 132:17840–17848. [PubMed: 21105659]
(19). Lee JE, Lee N, Kim T, Kim J, Hyeon T. Acc. Chem. Res. 2011; 44:893–902. [PubMed: 21848274]
(20). Hetrick EM, Shin JH, Stasko NA, Johnson CB, Wespe DA, Holmuhamedov E, Schoenfisch MH. ACS Nano. 2008; 2:235–246. [PubMed: 19206623]
(21). Hetrick EM, Shin JH, Paul HS, Schoenfisch MH. Biomaterials. 2009; 30:2782–2789. [PubMed: 19233464]
(22). Carpenter AW, Slomberg DL, Rao KS, Schoenfisch MH. ACS Nano. 2011; 5:7235–7244. [PubMed: 21842899]
(23). Jones ML, Ganopolsky JG, Labbe A, Wahl C, Prakash S. Appl. Microbiol. Biotechnol. 2010; 88:401–407. [PubMed: 20680266]
(24). Ghaffari A, Miller CC, McMullin B, Ghahary A. Nitric Oxide. 2006; 14:21–29. [PubMed: 16188471]
(25). Privett BJ, Broadnax AD, Bauman SJ, Riccio DA, Schoenfisch MH. Nitric Oxide-Biol. Ch. 2012; 26:169–173.
(26). Riccio DA, Schoenfisch MH. Chem. Soc. Rev. 2012; 41:3731–3741. [PubMed: 22362355]
(27). Carpenter AW, Schoenfisch MH. Chem. Soc. Rev. 2012; 41:3742–3752. [PubMed: 22362384]
(28). Shin JH, Metzger SK, Schoenfisch MH. J. Am. Chem. Soc. 2007; 129:4612–4619. [PubMed: 17375919]
(29). Koh A, Riccio DA, Sun B, Carpenter AW, Nichols SP, Schoenfisch MH. Biosens. Bioelectron. 2011; 28:17–24. [PubMed: 21795038]
(30). DeRosa F, Keefer LK, Hrabie JA. J. Org. Chem. 2008; 73:1139–1142. [PubMed: 18184006]
(31). Reynolds MM, Saavedra JE, Showalter BM, Valdez CA, Shanklin AP, Oh BK, Keefer LK, Meyerhoff ME. J. Mater. Chem. 2010; 20:3107–3114. [PubMed: 21132111]
(32). Riccio DA, Nugent JL, Schoenfisch MH. Chem. Mater. 2010; 23:1727–1735. [PubMed: 21499510]
(33). Coneski PN, Schoenfisch MH. Chem. Soc. Rev. 2012; 41:3753–3758. [PubMed: 22362308]
(34). Clogston, JD. NCL Method PCC-2: Measuring Zeta Potential of Nanoparticles. Nanotechnology Characterization Laboratory, N. C. I.. , editor. Frederick, MD: 2009.

(35). Breed RS, Dotterrer WD. J. Bacteriol. 1916; 1:321–331. [PubMed: 16558698]

(36). Shin JH, Schoenfisch MH. Chem. Mater. 2008; 20:239–249.

(37). Majumdar P, Lee E, Gubbins N, Christianson DA, Stafslien SJ, Daniels J, VanderWal L, Bahr J, Chisholm BJ. J. Combin. Chem. 2009; 11:1115–1127.

(38). Thorsteinsson T, Masson M, Kristinsson KG, Hjalmarsdottir MA, Hilmarsson H, Loftsson T. J. Med. Chem. 2003; 46

(39). Beyth N, Houri-Haddad Y, Baraness-Hadar L, Yudovin-Farber I, Domb AJ, Weiss EI. Biomaterials. 2008; 29:4157–4163. [PubMed: 18678404]

(40). Shi Z, Neoh KG, Kang ET, Wang W. Biomaterials. 2006; 27:2440–2449. [PubMed: 16338001]

(41). Malvern. Malvern Instruments, Ltd.; Worcestershire: 2007.

(42). Coneski PN, Schoenfisch MH. Org. Lett. 2009; 11:5462–5465. [PubMed: 19899748]

(43). Bjarnsholt T, Kirketerp-Møller K, Jensen PØ, Madsen KG, Phipps R, Krogfelt K, Høiby N, Givskov M. Wound Repair Regen. 2008; 16:2–10. [PubMed: 18211573]

(44). Privett BJ, Deupree SM, Backlund CJ, Rao KS, Johnson CB, Coneski PN, Schoenfisch MH. Mol. Pharmaceut. 2010; 7:2289–2296.

(45). Simoncic B, Tomsic B. Text. Res. J. 2010; 80:1721–1737.

(46). Silver S. FEMS Microbiol. Rev. 2003; 27:341–353. [PubMed: 12829274]

(47). Mohamed AF, Nielsen EI, Cars O, Friberg LE. Antimicrob. Agents Chemother. 2012; 56:179–188. [PubMed: 22037853]

(48). Wang J, Byrne JD, Napier ME, DeSimone JM. Small. 2011; 7:1919–1931. [PubMed: 21695781]

(49). Lv H, Zhang SW, Wang B, Cui S, Yan J. J. Control. Release. 2006; 114:100–109. [PubMed: 16831482]

(50). Lineaweaver W, McMorris S, Soucy D, Howard R. Plast. Reconstr. Surg. 1985; 75:394–396. [PubMed: 3975287]

(51). Thelestam M, Mollby R. Chem. Biol. Interact. 1980; 29:315–325. [PubMed: 7357678]

(52). Stasko NA, Johnson CB, Schoenfisch MH, Johnson TA, Holmuhamedov EL. Biomacromolecules. 2007; 8:3853–3859. [PubMed: 18004811]

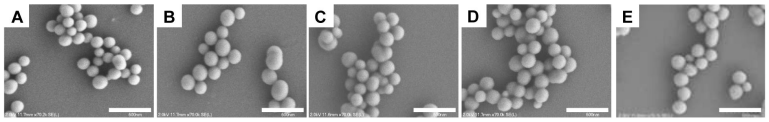

Figure 1.
Scanning electron micrographs of (A) AHAP (d=180±26 nm), (B) methylQA (d=181±27 nm), (C) butylQA (d=187±23 nm), (D) octylQA (d=185±26 nm), and (E) dodecylQA (d=187±24 nm) nanoparticles. Scale bar = 500 nm.

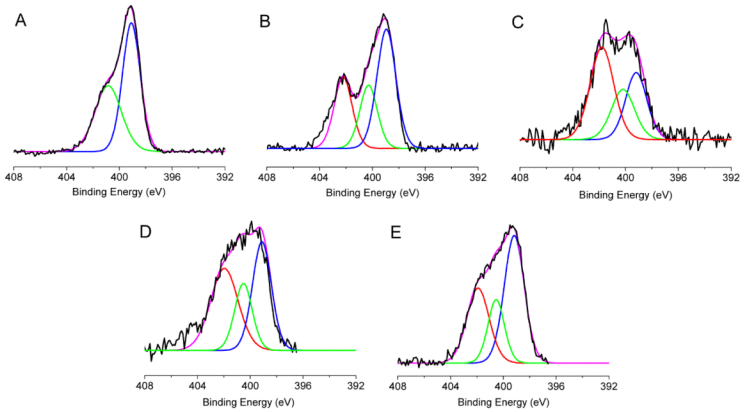

Figure 2.

X-ray photoelectron (XPS) spectra of the N 1s peak of (A) AHAP, (B) methylQA, (C) butylQA, (D) octylQA, and (E) dodecylQA nanoparticles. The presence of primary (blue), secondary (green) and quaternary (red) amines are indicated by fitted curves at binding energies of 399, 401, and 402 eV, respectively.

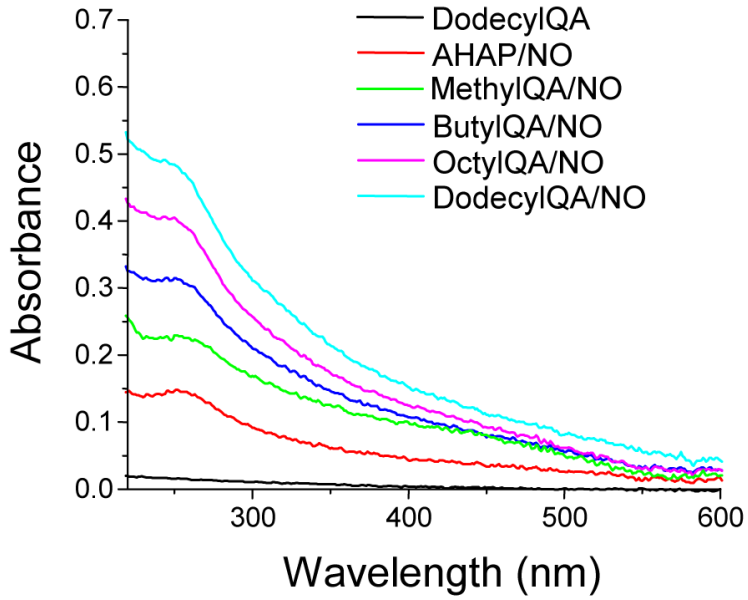

Figure 3.
UV-Vis absorbance spectra of *N*-diazeniumdiolate-modified AHAP and QA silica nanoparticles. Unmodified dodecylQA is shown for comparison.

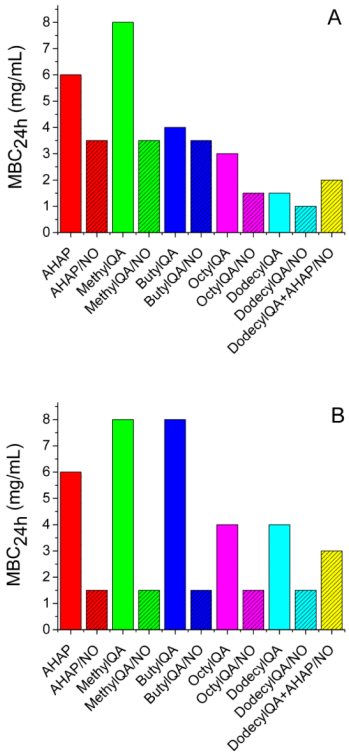

Figure 4.

Minimum bactericidal concentrations (MBC_{24h}) against (A) *S. aureus* and (B) *P. aeruginosa* for non-NO-releasing (solid) and NO-releasing (hashed) AHAP (red), methylQA (green), butylQA (blue), octylQA (magenta), dodecylQA (cyan). Treatment with a 50:50 (w/w) mixture of dodecylQA and AHAP/NO particles is shown in yellow (hashed).

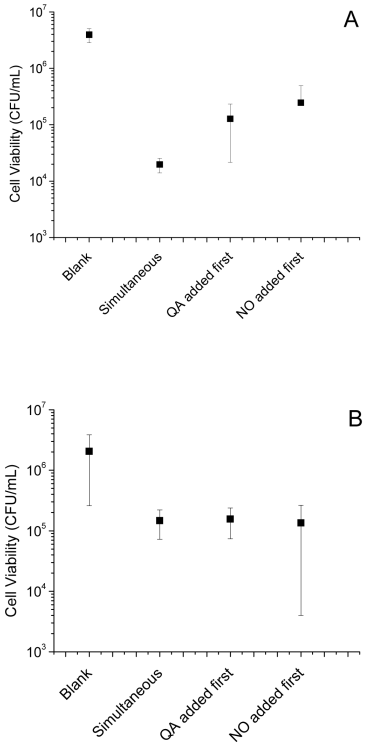

Figure 5.
Change in bacterial viability of (A) *S. aureus* and (B) *P. aeruginosa* following exposure to sublethal doses of dodecylQA and/or AHAP/NO nanoparticles either simultaneously or at 30 min intervals.

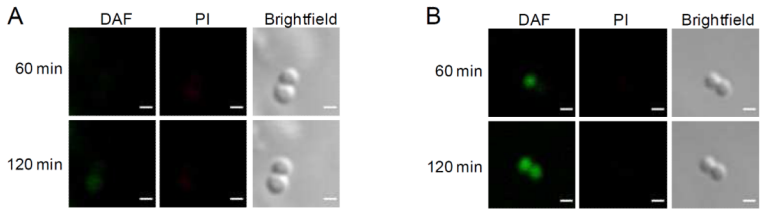

Figure 6.
Confocal microscopy images of *S. aureus* exposed to (A) dodecylQA/NO and (B) AHAP/NO particles exhibit green fluorescence due to intracellular NO (DAF) and red fluorescence due to compromised membrane (PI). Scale bar = 1 μm.

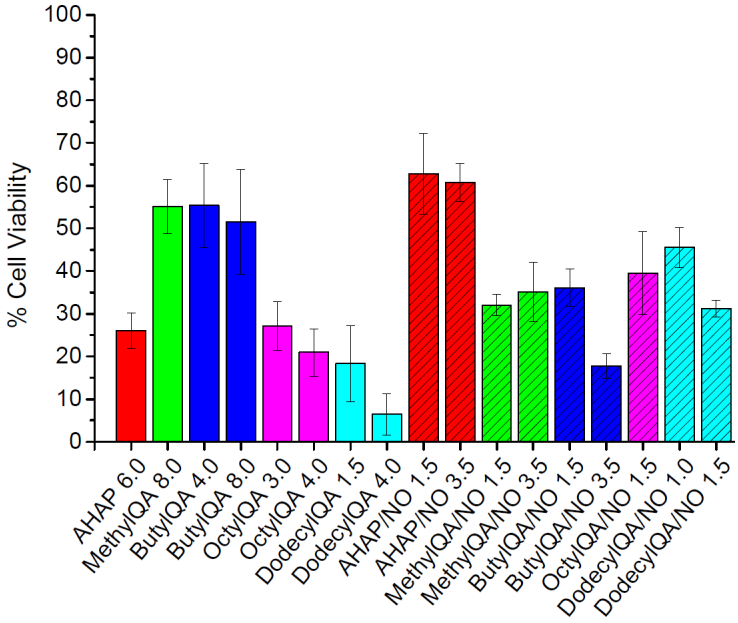

Figure 7.

Percent viability of L929 mouse fibroblasts cells following 24 h exposure to non-NO-releasing (solid) and NO-releasing (hashed) AHAP (red), methylQA (green), butylQA (blue), octylQA (magenta), and dodecylQA (cyan) particles compared to control (untreated) cells with the numbers corresponding to the MBC_{24h} against *S. aureus* and *P. aeruginosa* (in mg/mL dose).

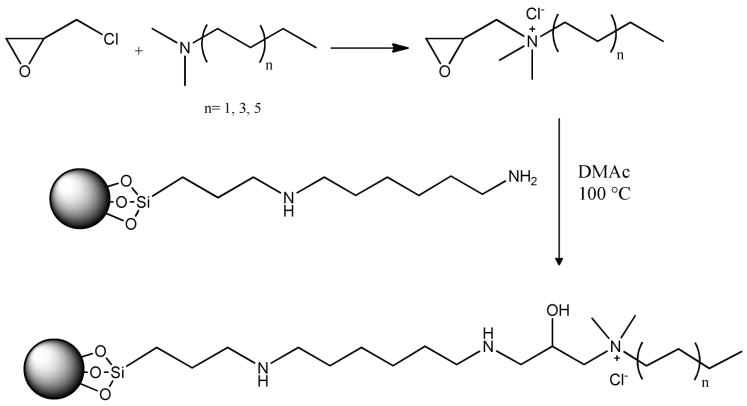

Scheme 1.

Quaternary ammonium (QA) epoxides were synthesized via reaction of epichlorohydrin with a dimethylalkylamine and subsequently reacted with the primary amines on the surface of AHAP/TMOS particles to yield QA-functionalized silica nanoparticles.

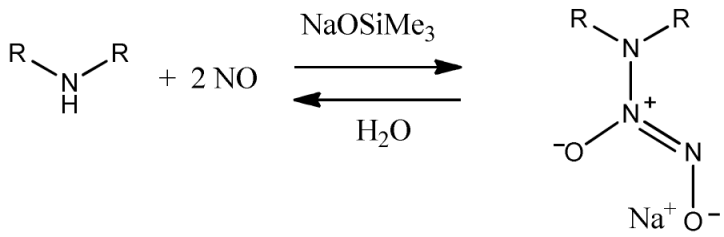

Scheme 2.

N-Diazeniumdiolate NO donors were formed on secondary amines within the particle upon exposure to high pressures of NO in the presence of a base (e.g., $NaOSiMe_3$). In the presence of a proton source (e.g., H_2O), these NO donors breakdown to regenerate the parent amine and two molecules of NO.

Table 1

Zeta potential measured from AHAP and QA-modified AHAP particle solutions.

	Zeta Potential (mV)	
	10 mM NaOH	**10 mM PB**
AHAP	−9.4±0.6	20.5±1.0
MethylQA	24.6±1.9	23.7±1.7
ButylQA	20.9±0.9	16.8±1.1
OctylQA	23.0±1.4	11.6±1.4
DodecylQA	22.8±0.6	19.8±0.6

Table 2

Nitric oxide release properties of unmodified and QA-modified silica nanoparticles, including total NO release ($[NO]_T$), maximum instantaneous concentration of NO ($[NO]_{max}$), and time to reach $[NO]_{max}$ (t_{max}).

	$[NO]_T$ (μmol/mg)	$[NO]_{max}$ (ppb/mg)	t_{max} (min)
AHAP/NO	0.27±0.04	1388±161	1.5±0.2
MethylQA/NO	0.30±0.03	1034±32	1.8±0.3
ButylQA/NO	0.27±0.03	882±36	2.3±0.2
OctylQA/NO	0.28±0.04	791±52	2.9±0.6
DodecylQA/NO	0.27±0.04	617±68	4.3±0.8